

Magnetic $\text{Fe}_{n+1}\text{AC}_n$ ($n = 1, 2, 3$, and $A = \text{Al, Si, Ge}$) phases: from *ab initio* theory

This article has been downloaded from IOPscience. Please scroll down to see the full text article.

2008 J. Phys.: Condens. Matter 20 064217

(<http://iopscience.iop.org/0953-8984/20/6/064217>)

View [the table of contents for this issue](#), or go to the [journal homepage](#) for more

Download details:

IP Address: 129.252.86.83

The article was downloaded on 29/05/2010 at 10:32

Please note that [terms and conditions apply](#).

Magnetic $\text{Fe}_{n+1}\text{AC}_n$ ($n = 1, 2, 3$, and $\text{A} = \text{Al, Si, Ge}$) phases: from *ab initio* theory

W Luo and R Ahuja

Physics Department, Condensed Matter Theory Group, Uppsala University, Box 530,
SE-751 21 Uppsala, Sweden

and

Applied Materials Physics, Department of Materials and Engineering, Royal Institute of
Technology (KTH), S-00 44 Stockholm, Sweden

Received 2 September 2007, in final form 5 November 2007

Published 24 January 2008

Online at stacks.iop.org/JPhysCM/20/064217

Abstract

We have investigated the structural stability and magnetism for a set of compounds $\text{Fe}_{n+1}\text{AC}_n$ ($n = 1, 2, 3$, and $\text{A} = \text{Al, Si, Ge}$) using *ab initio* theory. From our calculation, we have shown that some $\text{Fe}_{n+1}\text{AC}_n$ phases ($n = 2$) with the general MAX phase formula and a layered hexagonal structure that belongs to space group $D_{6h}^4-P6_3/mmc$ can have a combination of properties of the MAX phase at the same time as having magnetism. The Fe_3AlC_2 phase shows the most stable ferromagnetic properties among these MAX phases and the magnetic moment is $0.73 \mu_B/\text{Fe}$ atom. In addition, the phase stability is predicted by comparing the total energy of the Fe_2AlC and Fe_2SiC phases with the total energy of the competing equilibrium phases at the corresponding composition.

(Some figures in this article are in colour only in the electronic version)

The MAX phases consist of an early transition metal M in the periodic table, an element from the A groups, usually IIIA and IVA, and a third element X, which is either nitrogen or carbon, in the composition $\text{M}_{n+1}\text{AX}_n$, where n is 1, 2, or 3 [1]. These phases are in fact natural nanocomposites constituted of layers of a metal carbide or metal nitride interleaved with monatomic A element layers as shown in figure 1 [2]. This laminar structure provides the MAX phases with an extraordinary combination of mechanical and electric properties. Mechanically, they are readily machinable, relatively soft, and resistant to thermal shock and unusually damage tolerant [2]. Up to now more than 50 MAX phase compounds have been synthesized and there are more to be discovered [3]. The search for new combinations of MAX ceramics is still going on, in order to enable tuning of the properties of the MAX phase to obtain the optimum coating. An attempt is yet to be made to synthesize magnetic MAX phase. If one can make magnetic MAX phase compounds, they will be good functional materials. For example, they could be candidates for spintronics application. Due to the abundance of iron on Earth, a MAX phase with iron is a promising magnetic MAX phase compound candidate.

All MAX phases follow the general formula $\text{M}_{n+1}\text{AX}_n$, with a hexagonal structure that belongs to space group $D_{6h}^4-P6_3/mmc$ (194). The value of $n = 1, 2, 3$ gives the three reported crystal structures M_2AX , M_3AX_2 , and M_4AX_3 , respectively. These structures can be described as a nanolaminate with layers of a binary carbide or nitride MX interleaved with a single layer of A atoms. The structures of M_2AX and M_3AX_2 phases comprise slabs of distorted edge sharing MX_6 octahedra separated from each other by layers of the A group element. The insertion of A layers means that M–A bonds replace M–X bonds.

In this paper we present first-principles calculations for the magnetic MAX phase. The electronic structure has been calculated using the Vienna *ab initio* simulation package VASP. VASP performs a variational solution of the Kohn–Sham equations of density functional theory (DFT) in a plane-wave basis, using a projector-augmented-wave (PAW) technique for describing the electron–ion interaction. VASP also offers the possibility of optimization of the idealized structure derived from the MAX phase model by relaxing all atomic coordinates to equilibrium positions while preserving the space group symmetry. The following parameters are used: 0.01 eV

Table 1. Calculated crystal constants, bulk moduli, and magnetic moments for $\text{Fe}_{n+1}\text{AC}_n$, as well as the energy difference between nonmagnetic and ferromagnetic; antiferromagnetic and ferromagnetic. A positive value implies a stable ferromagnetic phase against the nonmagnetic or antiferromagnetic phase.

| Phase | c (Å) | c/a | B (GPa) | B'_0 | $\Delta E(\text{nf})$ (meV/f.u.) | $\Delta E(\text{af})$ (meV/f.u.) | μ_B/iron | Synthesized c/a [2] |
|---------------------------|---------|-------|-----------|--------|-------------------------------------|-------------------------------------|----------------------|--------------------------|
| Fe_2AlC | 11.9347 | 4.2 | 164 | 4.2 | 125 | -97 | 4f: 1.18 | 3.5–4.6 |
| Fe_3AlC_2 | 16.1348 | 5.5 | 173 | 4.2 | 190 | 190 | 2a: 1.44 4f: 0.38 | 5.7–6 |
| Fe_4AlC_3 | 20.0648 | 6.8 | 179 | 4.8 | 72 | 0 | 4e: 0.18 4f: 0.86 | 7.8 |
| Fe_2GeC | 11.4527 | 3.9 | 172 | 4.6 | 32 | -20 | 4f: 0.96 | |
| Fe_3GeC_2 | 15.7553 | 5.3 | 176 | 4.7 | 119 | -3 | 2a: 1.57 4f: 0.39 | |
| Fe_4GeC_3 | 19.9064 | 6.7 | 211 | 4.6 | 53 | -10 | 4e: 0.17 4f: 0.84 | |
| Fe_2SiC | 11.6005 | 4.1 | 183 | 5.0 | 0 | -35 | 4f: 0.71 | |
| Fe_3SiC_2 | 15.5317 | 5.3 | 186 | 5.1 | 47 | 0 | 2a: 1.40 4f: 0.30 | |
| Fe_4SiC_3 | 19.9254 | 6.8 | 200 | 5.2 | 23 | -11 | 4e: 0.08 4f: 0.77 | |

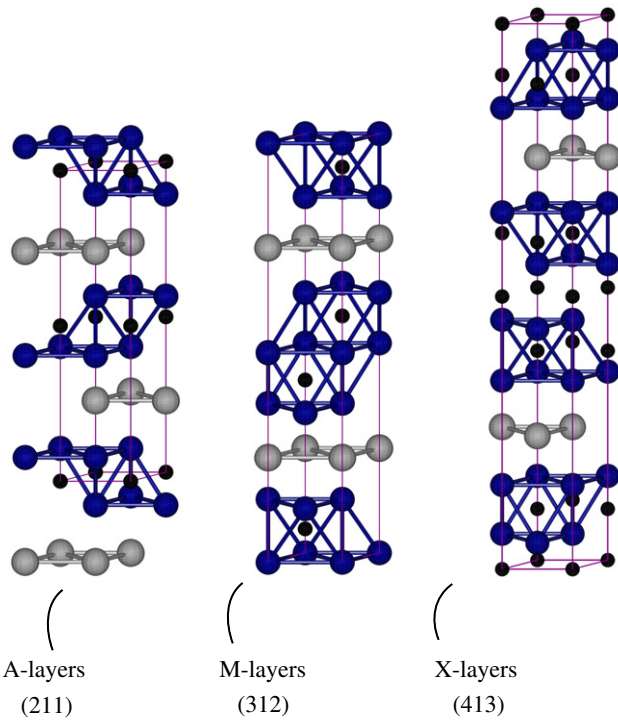


Figure 1. The hexagonal crystal structures for the $\text{M}_{n+1}\text{AX}_n$ phases ($n = 1, 2$ or 3 ; taken from [2]) showing the different stackings in the existing subgroups of the compositions M_2AX , M_3AX_2 and M_4AX_3 . For example: in a 211 phase, the A elements are separated by a layer of transition metal carbide or nitride of formula M_2X whereas in a 312 phase, the A element atoms are separated by transition metal carbide or nitride of formula M_3X_2 . Most of the MAX phases known today belong to the 211 class.

relaxation convergence for ionic positions, 0.1 meV electronic relaxation convergence, energy cut-off of 875 eV, k -point grid of $7 \times 7 \times 1$. The calculations are carried out using the generalized gradient approximation (GGA) for the exchange and correlation potential as described by Perdew, Burke and

Ernzerhof. For the calculations reported here, we have used semicore 3p states as well as 3d and 4s states of Fe as valence states, 2s and 2p states as valence states for C, 3s and 3p states for Al and Si, and 4s and 4p states for Ge. In our computations, the tetrahedron method with Blöchl corrections is used to calculate the total energy and density of states (DOS). The lattice constants and the bulk moduli (B) are evaluated from the Birch–Murnaghan fit to the total energies as a function of the unit cell volume.

All $\text{Fe}_{n+1}\text{AC}_n$ phases are assumed to have the general MAX phase formula with a layered hexagonal structure that belongs to space group $P6_3/mmc$. The structures are relaxed with respect to the parameter a , c/a and internal positional parameters. The bulk modulus is calculated by fitting the energy–volume curve using the Birch–Murnaghan equation of states. The results for the ground state volume, lattice geometry, and bulk moduli of $\text{Fe}_{n+1}\text{AC}_n$ ($n = 1, 2, 3$, and $A = \text{Al, Si, Ge}$) are listed in table 1. The calculation for the unit cell parameters indicates a shorter c -axis of $\text{Fe}_{n+1}\text{AC}_n$ phases with increasing n , unlike all other $\text{M}_{n+1}\text{AC}_n$ phases known to date. The unit cell parameters and lattice geometry for all of the Fe_2AC ($A = \text{Al, Si, Ge}$) compounds appear to be comparable to those determined and calculated for other M_2AX compounds. The c/a ratio of Fe_2AC compounds varies from 3.9 to 4.4, in the range of 3.5–4.6 for the known M_2AX [2]. The bulk moduli of $\text{Fe}_{n+1}\text{AC}_n$ increase with n increasing from 1 to 3, as well as with the element A of the single layer implanted in the $\text{Fe}_{n+1}\text{AC}_n$ phases changing from Al to Ge to Si. In order to investigate the ferromagnetic stability, we compare total energies of ferromagnetic phase with the nonmagnetic and the antiferromagnetic phases. The total energy differences between these phases are calculated and listed in table 1. The positive energy difference compared to the nonmagnetic phase, i.e. $\Delta E(\text{nf})$, or of the antiferromagnetic phase, i.e. $\Delta E(\text{af})$, with respect to the ferromagnetic phase indicates the stability of the ferromagnetic phase. Our results indicate that only Fe_3AlC_2 shows stable ferromagnetic behavior and an

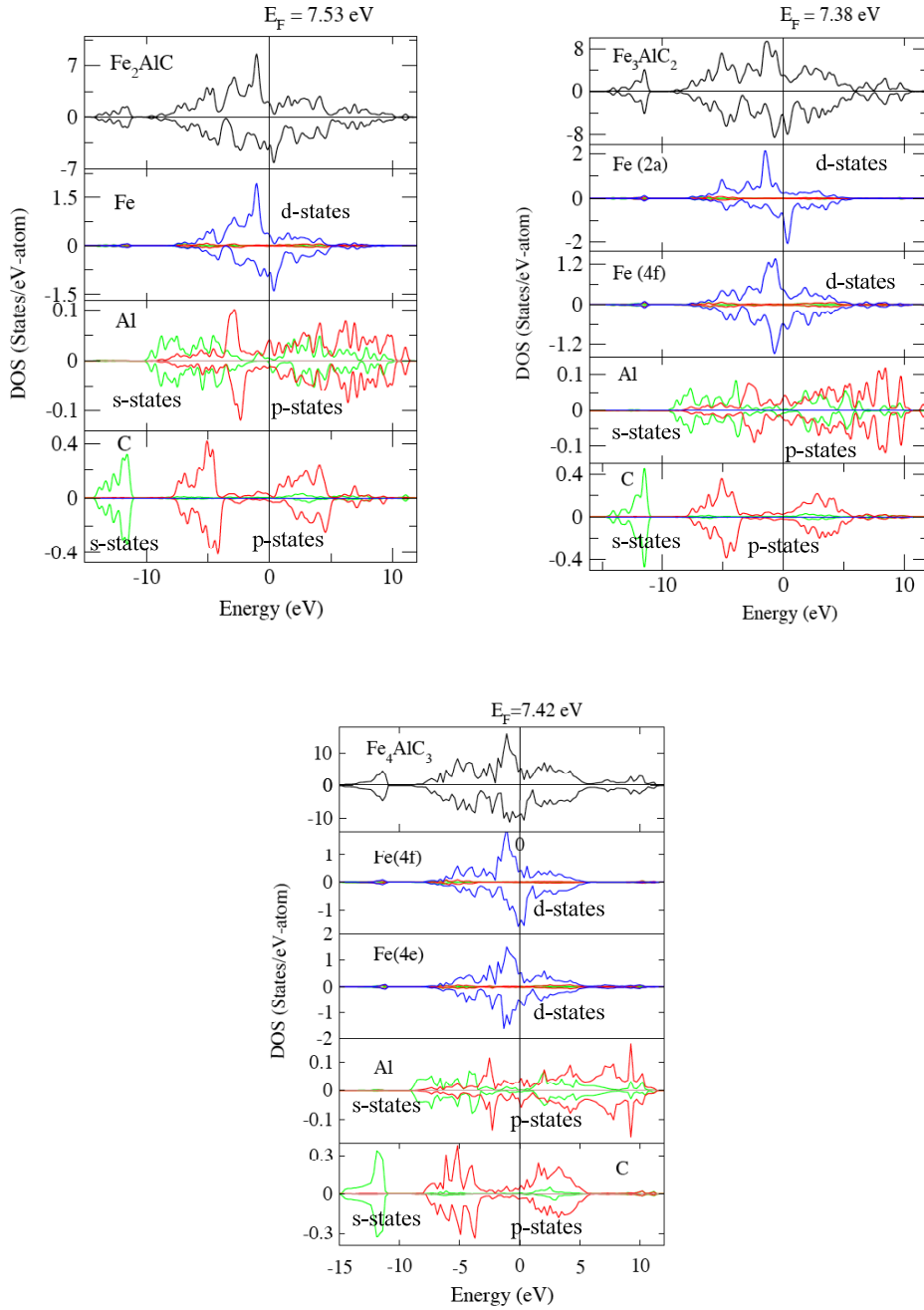


Figure 2. Total DOS and PDOS (a) for the Fe_2AlC , (b) for Fe_3AlC_2 , and (c) for Fe_4AlC_3 ferromagnetic phases.

average moment up to $0.73 \mu_B/\text{Fe}$ atom. The iron in different symmetry position shows different magnetic moments because of connecting with different atoms in the stacking sequence. The iron atoms in Fe_2AC compounds possess only one equivalent position, the 4f site, so they show unique magnetic moments. Our calculations show that the Fe_2AC phase exhibits a much stronger magnetic moment, $1.18 \mu_B/\text{Fe}$ atom than those of Fe_2GeC and Fe_2SiC . The structure of Fe_3AC_2 can be described as hexagonal layers stacked in the repeated sequence of A–Fe–C–Fe–C–Fe slabs [4–6]. There are two inequivalent Fe layers: Fe(I) atoms at 2a position layers with a C layer on one side and an A layer on the other, showing a large magnetic moment; and Fe(2) layers at 4f sites which are

sandwiched between two C layers, presenting a low magnetic moment. These typical characteristics are observed in Fe_4AC_3 as well. The stacking sequence refers to the Fe(II), 4e positions between two C layers. As shown in table 1, the magnetic moment of iron at the 4e site is much weaker than that of Fe(I) at the 4f site, indicating the different coupling of electrons at different sites.

The phase equilibrium and thermodynamic analysis of the phase diagram for the Fe–Al–C alloy ternary system have been studied without the MAX phase field [7–9]. In order to check the stability of the magnetic MAX phase, we have checked the phase diagram of the Fe–A–C (A = Al, Si, Ge) system. During the sintering of $\text{M}_{n+1}\text{AlC}_n$ phases, Al_4C_3 is often adopted

as a starting material owing to the ease of getting the MAX compounds [10, 11]. The structure of Al_4C_3 is crystallized rhombohedral $R\bar{3}m$, which is closely related to the structure of the MAX phase. So we consider the phases competing with Fe_2AlC to be Al_4C_3 , Fe_3C , and Fe. The reaction equation is



and their calculated total energies (in eV per atom) are -7.39 , -6.19 , -8.38 , and -7.70 , respectively. The results show that there is a negative energy difference of -0.18 eV/atom between the Fe_2AlC phase and its competing phases. This suggests that the Fe_2AlC phase can be stabilized.

Since the first observation of the Fe–C diagram in 1908, thermodynamic calculations for stable and unstable phases of the Fe–Si–C system [12, 13] have been reported. One can note from these works that most of the Fe–C and related phase diagrams were established on the basis of cast iron metallurgy [14]. Therefore, the attempts to apply the currently known Fe–C and Fe–C–Si diagrams to the analysis of solidification of Fe–C–Si system are fraught with difficulty. We deduce the energies of cohesion of the competing phases of Fe_2SiC , which are Fe and SiC. The following reaction is studied:



A negative formation energy of Fe_2SiC is observed which means that Fe_2SiC is stable against its competing phases. The total energy per atom is -7.73 eV for Fe_2SiC , -7.54 eV for 6H-SiC , and -7.70 eV for bcc Fe. The energy difference between Fe_2SiC and the competing phases is -0.41 eV for the chemical reaction formula. In fact, some observed MAX compounds are unstable towards the competing phases [15]. It is reasonable to suggest that the Fe–Si–C MAX phases can be formed as metastable compounds and may be synthesized as thin films.

In order to analyze the electronic structure of $\text{Fe}_{n+1}\text{AlC}_n$ phases, we calculate the density of states and partial density of states (DOS) of Fe_2AlC , Fe_3AlC_2 , and Fe_4AlC_3 phases, as presented in figures 2(a)–(c), respectively. The lowest lying states positioned around -10 eV, originated from the C 2s states; Al 3s states contribute to the states between -9 and -6 eV. The states just below the Fermi level (E_f) (-6 – 0 eV) are dominated by hybridized Fe 3d orbital and C 2p states. The DOS of Fe_2AlC is not very similar to that of Ti_2AlC [16]. The states at the Fermi level are mainly Fe d and Al p. Carbon does not contribute significantly to the DOS at the Fermi level and therefore is not involved in the conduction properties. The density of states for Fe_3AlC_2 is very similar to that of Fe_2AlC . The Fe d–Al p bonds are stronger in Fe_2AlC than in Fe_3AlC_2 . Completely different from that of the Fe atom at the 4f site in

Fe_3AlC_2 phase, the partial DOS of Fe at the 2a site in Fe_3AlC_2 is quite similar to that of the Fe at the same symmetry 4f site in the Fe_2AlC phase. The ferromagnetic behaviors in 312 phases are mainly contributed by the Fe atoms at 2a sites.

In conclusion, we use *ab initio* calculations to calculate the crystal geometry, bulk moduli, and magnetic moments of $\text{Fe}_{n+1}\text{AlC}_n$ ($n = 1, 2, 3$, and A = Al, Si, Ge) phases. Our results show the stability of Fe_2AlC and Fe_2SiC MAX phases. So we predict materials which could have a combination of properties of MAX phases, at the same time having magnetism. We welcome experiments to check our predictions.

Acknowledgments

We thank the Swedish Research Council (VR) and SIDA for financial support.

References

- [1] Barsoum M W and El-Raghy T 2001 *Am. Sci.* **89** 334
- [2] Barsoum M W 2000 *Prog. Solid State Chem.* **28** 201
- [3] Barsoum M W, El-Raghy T and Radovic M 2000 *Interceram* **49** 226
- [4] Stoltz S E, Starnberg H I and Barsoum M W 2003 *J. Phys. Chem. Solids* **64** 2321
- [5] Amer M, Barsoum M W, El-Raghy T, Weiss I, Leclair S and Liptak D 1998 *J. Appl. Phys.* **84** 5817
- [6] Rawn C J, Barsoum M W, El-Raghy T, Prociopio A, Hoffmann C M and Hubbard C R 2000 *Mater. Res. Bull.* **35** 1785
- [7] Shankar Rao V 2004 *J. Mater. Sci.* **39** 4193
- [8] Pozdova T and Golovin I 2003 *Solid State Phenom.* **89** 279
- [9] Yang S H, Mehl M J, Papaconstantopoulos D A and Scott M B 2002 *J. Phys.: Condens. Matter* **14** 1895
- [10] Zhou A, Wang C-A and Huang Y 2003 *Mater. Sci. Eng. A* **352** 333
- [11] Barsoum M W, Salama I, El-Raghy T, Golczewski J, Porter W D, Wang H, Seifert H J and Aldinger F 2002 *Metall. Mater. Trans. A* **33** 2775
- [12] Sigfússon P I, Gylfason G H and Sveinsdóttir E L 1990 Rannsóknir á steindalíti I-III, RH-05-90 og RH-06-90 *Research into Steindalite, Fe–Si–C Ceramics, Reports* <http://www.raunvis.hi.is/~this/research.htm#Layercastingofferrosilicon>
- [13] Miettinen J 1998 Reassessed thermodynamic solution phase data for Fe–Si–C system *CALPHAD* **22** 231
- [14] Miettinen J 1997 Thermodynamic description of liquid, bcc and fcc phases of ternary Fe–Si–C system *Report TKK-MK-30* Laboratory of Metallurgy, Helsinki University of Technology, p 26
- [15] Aaronson H I 1986 *Metall. Trans. A* **17** 1095
- [16] van de Velde C <http://members.lycos.nl/cvdiv/fecdiagram.htm>
- [17] Grechnev A, Li S, Ahuja R, Eriksson O, Jansson U and Wilhelmsson O 2004 *Appl. Phys. Lett.* **85** 3071
- [18] Hug G and Fries E 2002 *Phys. Rev. B* **65** 113104